Feedback Control Using Shape Memory Alloy Actuators

CARRIE A. DICKINSON AND JOHN T. WEN*

Center for Automation Technologies, Department of Electrical, Computer, and Systems Engineering, Rensselaer Polytechnic Institute, 110 8th Street, Troy, NY 12180-3590

ABSTRACT: Shape memory alloy (SMA) has been considered as an actuator for applications that require large force and displacement. Two factors have hampered the usefulness of such actuators: a hysteretic input-output relation and bandwidth limitations. This paper considers the hysteresis phenomenon from a control point of view. Instead of directly compensating for the hysteresis, which requires an accurate model, we use a closed loop approach which considers the feedback control of the beam strain. A simple lumped temperature and SMA force/displacement model is used for stability analysis. We show that with the SMA wire fixed between rigid surfaces, a proportional force feedback would render the closed loop stable. However, when SMA is coupled to a flexible structure, the resulting system can exhibit instability. We then show that a proportional *position* feedback is stabilizing, but there would be steady-state error. An adaptation scheme can be further added to remove the steady-state error. The analysis is verified experimentally in a simple experimental setup consisting of a flexible aluminum beam and a Nitinol shape memory alloy wire that applies a bending force to the end of the beam.

INTRODUCTION

SHAPE memory alloys are materials which have the ability to "remember" their shape even after large deformations. Once deformed at a low temperature (in a martensitic phase), an SMA will remain deformed until heated, when it returns to the original austenitic phase. SMA can be used as an actuator: applied thermal energy causes internal phase transformation (between austenitic and martensitic phases) which in turn generates a mechanical strain. Although large force and displacement can be realized with these actuators, the effectiveness of SMA actuators is typically hampered by two factors:

1. Hysteresis: The phase transformation is a hysteretic phenomenon (similar to that of ferromagnetic materials) resulting in the output strain dependent on the history of heat input.
2. Bandwidth Limitation: Due to the typically large heat transfer time constant, the dynamic response of an SMA actuator is very slow.

This paper addresses the hysteresis of SMA from a control perspective. Generally speaking, there are two types of approaches to deal with hysteretic nonlinearity:

1. Open Loop Compensation: Find a first-principle or phenomenological model, identify the parameters, then invert the model, if possible, to remove or at least ameliorate the nonlinearity.
2. Closed Loop Feedback: Use the output error (measured output subtracting the desired output) to generate the corrective heat input. The output may be the force applied by the SMA wire, or the position, or the strain of the structure to which the SMA wire is connected.

We will describe our recent work on closed loop feedback compensation of SMA hysteresis.

Because of their light weight and ability to produce large force and displacement, SMA actuators have been used in a wide range of applications including large space structures, robotic arms, medical instruments, and surgical implants. SMA are commonly used with flexible structures for shape control, vibration suppression, and tracking control (Baz et al., 1990, Ikegami et al., 1990, Dickinson et al., 1996). However, there has been very little work done in controlling SMA, primarily because they are assumed to be essentially static devices. In terms of open loop modeling of the SMA hysteresis, the Preisach model has often been chosen because of its simple structure, easy identifiability, invertibility, and implementability for both simulation and control (Hughes and Wen, 1995). Recently, a passivity based approach has been used to analyze closed loop stability involving SMA (Madill and Wang, 1994), and a variable structure type of controller has also been successfully applied (Grant and Hayward, 1997).

This paper builds on our previous work in Dickinson et al. (1996) considering controlling a flexible beam with an externally attached SMA wire at the tip of the beam. Simplification of the model developed in Shu et al. (1997) has been used for stability analysis. It has been shown in Dickinson et al. (1996) and Dickinson (1997) that force feedback for a single fixed SMA wire is stable by using the Circle Criterion (Vidyasagar, 1993). When the SMA wire is attached to a flexible beam, force feedback can now lead to instability. In this paper, we show that a simple nonlinear strain-feedback control law is stable. In this control law, a static nonlinear map between the desired beam strain and a fictitious desired

*Author to whom correspondence should be addressed.

1045-389X/98/04 0242-09 $10.00/0

strain needs to be established experimentally. Furthermore, we show that this fictitious desired strain can be adaptively updated and obtain a general condition for stability again by using the Circle Criterion. Experiments have been conducted to demonstrate the validity of our analysis.

EXPERIMENTAL SETUP AND DYNAMIC MODEL FOR A BEAM WITH EXTERNALLY ATTACHED SMA WIRE

Figure 1 is an outline of the single-link flexible beam testbed used in our investigation. The central component is a flexible beam which is chosen to provide readily measurable flexibility in the horizontal plane that is independent of gravity (ideally). This beam is driven by a Nitinol SMA wire attached between the hub and the free end of the beam.

The SMA wires consist of 0.008″ thick Nitinol wires, approximately 1.09 m long. These are Flexinol wires made by Dynalloy with a characteristic transition temperature given as 90°C and a maximum pull force of 590 g, approximately. A complication of this configuration is that the wire stress is a function of the wire strain (and thus the beam strain), and so independent control of these two variables is not possible once the wire is connected unless an external force is applied, e.g., by use of weighted pulley wheel, or by use of a second SMA wire muscle on the other side of the beam. We have also included some results using the two-SMA-wire push-pull type of arrangement. A model of this setup has been developed in Shu et al. (1997).

To analyze the closed loop behavior, we approximate the temperature evolution in the wire by a lumped model for the average SMA wire temperature with convective cooling and resistive heating:

$$\dot{T} = -\alpha(T - T_r) + \beta u^2 \tag{1}$$

where the cooling coefficient $\alpha = [4h(T,D)/C_v(T)D]$ (with D, $h(T,D)$, and $C_v(T)$ the diameter, free heat convection coefficient, and heat capacity of SMA, respectively), the heating coefficient $\beta = [\rho_e/C_v(T)A^2]$ (with ρ_e the electrical resistivity and A the area of the SMA wire), T_r is room temperature, and u is the commanded current through the SMA wire. The resistive heating of the wire causes the phase transformation in the SMA.

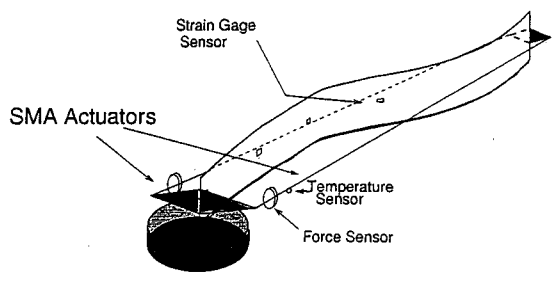

Figure 1. *Experimental testbed schematic.*

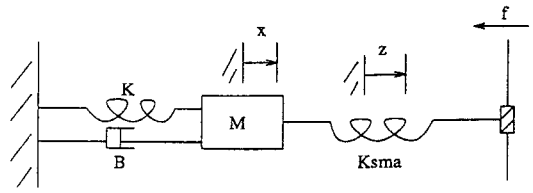

Figure 2. *Approximate lumped model for SMA wire connected to a mass-spring-damper system.*

We approximate the beam by one mode, i.e., a single mass-spring-damper system with mass M, damping coefficient B, and spring constant K. The phase transformation is modeled as an internal lumped displacement, z, as shown in Figure 2. Although we use a one-mode approximation for the beam model, we believe that the following analysis would be true for a more detailed beam model as well since the Circle Criterion type argument would remain valid.

Under the above assumption, the dynamical equation of the beam is

$$M\ddot{x} + B\dot{x} + Kx = f \tag{2}$$

where $x = -L_{sma}\varepsilon$ denotes the displacement of the flexible mode (with L_{sma} and ε the length and strain of the SMA, respectively), and the measured force, f, is given by

$$f = K_{sma}(z - x) \tag{3}$$

where $K_{sma} = (E_{sma}A/L_{sma})$ is the stiffness of the SMA wire (with E_{sma} as the Young's modulus).

The internal displacement, z, is related to the temperature by the function

$$z = L_{sma}(\varepsilon^t + \alpha_1(T - T_r)) \tag{4}$$

with ε^t the transformation strain of the SMA and α_1 the thermal expansion coefficient.

The strain ε, stress σ, and temperature T are related by the following set of equations:

$$\varepsilon^t = H\xi \tag{5}$$

$$\dot{\sigma} = \frac{\dot{f}}{A} \tag{6}$$

$$\sigma H + \frac{1}{2}\Delta s\sigma^2 + \Delta\alpha_1\sigma(T - T_r) + \rho\Delta s_0 T - \rho b\xi - Y^{**} = 0 \tag{7}$$

where H is the prestrain of SMA, ξ the martensite fraction, $\Delta s = (1/E^M) - (1/E^A)$ the elastic compliance difference, $\Delta\alpha_1 = \alpha^M - \alpha^A$ the thermal expansion coefficient difference, $\rho\Delta s_0$

the entropy difference at the reference state, ρb the isotropic hardening term, and Y^{**} the threshold value of transformation. The above equations are valid for both forward and reverse transformation, but the parameter values for $\rho\Delta s_0, \rho b$, and Y^{**} depend on the direction of the phase transformation. This accounts for the hysteresis exhibited in shape memory alloys.

Thus, the internal displacement z of Equation (4) is related to the temperature, stress, and strain through a general hysteresis function

$$z = g(T, \varepsilon, \sigma) = \begin{cases} g_u(T, \varepsilon, \sigma), & \dot{T} > 0 \\ g_d(T, \varepsilon, \sigma), & \dot{T} < 0 \end{cases} \tag{8}$$

where g_u and g_d are two scalar monotonically increasing functions with g_u lying strictly below g_d for the same range of T.

POSITION FEEDBACK CONTROL

To compensate for the hysteresis through static open-loop inversion is approximate at best, and involves careful experimentation for parameter identification off-line. We explore the feedback control approach in this section. Feedback control for SMA has not been extensively explored in the literature, mainly due to the assumption that the low bandwidth character of SMA renders it essentially a static device. We have shown in Dickinson et al. (1996) that the dynamic response cannot be ignored. Sampling rate in a sample-data implementation greatly affects the steady state oscillation, and, in certain configurations, even small feedback gains can lead to instability. In terms of stability analysis, a passivity approach has been proposed to show closed loop stability of a simple SMA feedback experiment using the proportional feedback (Madill and Wang, 1994). In Dickinson et al. (1996) we use a phase plane based argument for the stability of a simple proportional feedback system. We verified our results experimentally, but we still observed sizable steady state oscillation.

In this section, we will demonstrate that the control law in Dickinson et al. (1996) can be modified in simple ways to render the closed loop system stable. The Circle Criterion is applied to show the closed loop stability even for a general hysteresis model as given in Equation (8).

In Dickinson et al. (1996) we have considered the following control law which is essentially proportional feedback:

$$u^2 = \begin{cases} 0, & x > x_d \\ k(x_d - x), & x < x_d \end{cases} \tag{9}$$

where k is a non-negative gain chosen by the designer, x is the measured beam deflection, and x_d is the desired beam deflection. The motivation of this control law is straightforward: if the position output is below the setpoint, apply more heat to the wire, if the position output is above the setpoint, remove heat and let the spring in the system pull the beam back. In experimenting with this control law, we observed that for k relatively small, x would reach a steady state below the setpoint. When k is increased, the steady state error reduces and eventually fall into a limit cycle about the setpoint.

The closed loop behavior observed with the controller Equation (9) is due to the fact that x_d does not correspond to the steady state of the closed loop system. Let the steady state temperature and spring displacement be (T^*, x^*). Then from Equations (1) and (2), we have

$$T^* = \frac{\beta k_s}{\alpha}(x_d - x^*) + T_r \tag{10}$$

$$\bar{K}x^* = K_{sma}\, g(T^*, \varepsilon^*, \sigma^*) \tag{11}$$

where $\bar{K} = K + K_{sma}$, and $(\varepsilon^*, \sigma^*)$ are the steady state strain and stress in the SMA wire. We assume that when $T = T^*$, $\varepsilon = \varepsilon^*$ and $\sigma = \sigma^*$. This assumption simplifies our stability analysis. Though it is not true in general, it is a reasonable approximation since g usually does not strongly depend on ε and σ.

In Equation (10), to include both the heating and cooling in the analysis, we use a nonlinear gain k_s to denote the gain switching between the two cases:

$$k_s = \begin{cases} k, & x < x_d \\ 0, & x > x_d \end{cases} \tag{12}$$

Defining the error variables as

$$\delta x = x - x^* \tag{13}$$

$$\delta T = T - T^* \tag{14}$$

Equations (2) and (1) become

$$M\delta\ddot{x} + B\delta\dot{x} + \bar{K}\delta x = K_{sma}[g(T, \varepsilon, \sigma) - g(T^*, \varepsilon^*, \sigma^*)] \tag{15}$$

$$\delta\dot{T} = -\alpha\delta T - \beta k_s \delta x \tag{16}$$

The closed loop system is shown in the block diagram form in Figure 3. The error system can be written in the following compact form:

$$\begin{aligned} \dot{X} &= AX + BV \\ Y &= CX \\ V &= \phi(Y) = -(g(Y + T^*, \varepsilon, \sigma) - g(T^*, \varepsilon^*, \sigma^*)) \end{aligned} \tag{17}$$

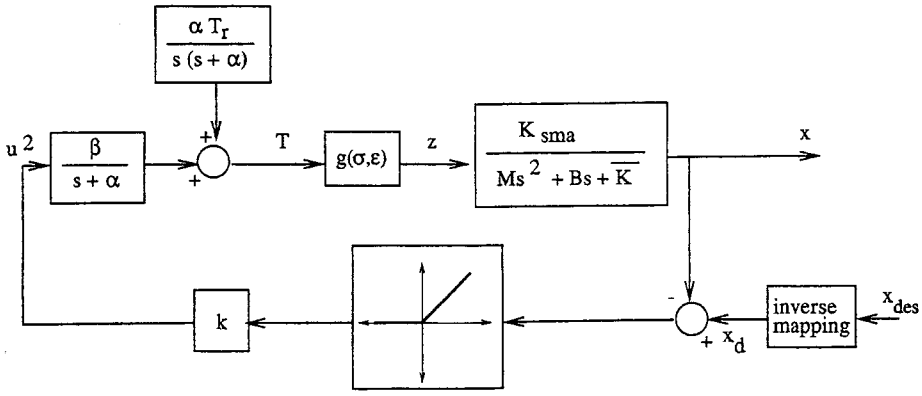

Figure 3. *Feedback block diagram of closed loop system with fixed* x_d.

where

$$X = \begin{bmatrix} \delta T \\ \delta x \\ \delta \dot{x} \end{bmatrix}, \quad A = \begin{bmatrix} -\alpha & -\beta k_s & 0 \\ 0 & 0 & 1 \\ 0 & -\frac{K}{M} & -\frac{B}{M} \end{bmatrix},$$

$$B = \begin{bmatrix} 0 \\ 0 \\ -\frac{K_{sma}}{M} \end{bmatrix}, \quad C = [1 \quad 0 \quad 0] \tag{18}$$

All of the eigenvalues of A are stable:

$$\text{eigenvalues}(A) = \left\{-\alpha, -\frac{1}{2M}(B + \sqrt{B^2 - 4M\bar{K}}), \right.$$

$$\left. -\frac{1}{2M}(B - \sqrt{B^2 - 4M\bar{K}})\right\}$$

The closed loop system exactly fits the form of the classic Lur'e Problem (Vidyasagar, 1993) (see Figure 4).

For SMA, the derivative of g with respect to T is typically bounded between two positive numbers:

$$0 \le a \le \frac{\partial g}{\partial(\delta T)} \le b \tag{19}$$

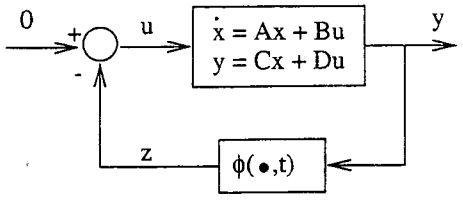

Figure 4. *Feedback control system describing the Lur'e Problem.*

over the range of possible ε and σ. It then follows that ϕ is sector bounded in $[a,b]$:

$$a|\delta T|^2 \le \phi(\delta T)\delta T \le b|\delta T|^2 \tag{20}$$

A sufficient condition for the global closed loop asymptotic stability is given by the Circle Criterion (Vidyasagar, 1993) which states that the Nyquist plot of

$$G(s) = C(sI - A)^{-1}B$$

$$= \beta k_s K_{sma}(s + \alpha)^{-1}(Ms^2 + Bs + \bar{K})^{-1} \tag{21}$$

has to remain outside of the disk that is symmetric about the real axis and intersecting the real axis at $[-(1/a), -(1/b)]$. The general shape of the Nyquist plot of G is shown in Figure 6. Clearly, if k_s (fixed as a constant gain) is sufficiently small, the closed loop system is asymptotically stable. As defined in Equation (12), k_s is either 0 or k depending on the sign of $(x - x_d)$. When $k_s = 0$ (i.e., $x > x_d$), the system is always stable. Physically, this corresponds to the control being shut off, and the spring restoration force of the flexible beam brings x back toward x_d. When $k_s = k$ (i.e., $x < x_d$), the system would be sta-

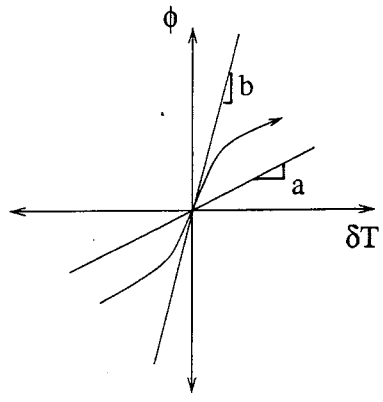

Figure 5. *Sector-bounded nonlinearity* ϕ.

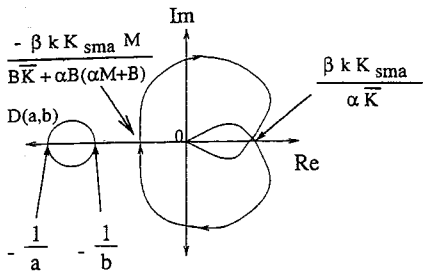

Figure 6. *Circle criterion for controller with fixed* x_d.

ble provided k is sufficiently small. Physically, this means that the SMA wire is heated and the contractive force increases x toward x_d.

Summarizing the discussion above, the following design procedure is proposed for a globally asymptotically stabilizing controller given by Equation (9).

1. Choose a feedback gain k sufficiently small to ensure stability.
2. For the chosen k, experimentally characterize the $x_d \to x^*$ mapping (stored as a table).
3. Find the inverse of the mapping from the previous step.
4. Apply the SMA controller as described in Equation (9). Then $x \to x^*$ in the steady state.

In a sample-data implementation, we still expect a certain amount of steady-state oscillation which should reduce in amplitude with increasing sampling frequencies.

ADAPTIVE CONTROLLER

In the controller presented in the previous section, the mapping from x_d to x^* has to be generated for each specified value of k. Since the precise model parameters for SMA are rarely available, the mapping would need to be obtained experimentally. This is clearly problematic if one needs to tune the feedback gain k for the desired performance. In this section, we propose a simple adaptation strategy that estimates x_d rather than using the pre-computed x^* to x_d mapping. The motivation is simple, if x is below x^*, then x_d should increase, and, conversely, if x is above x^*, then x_d should decrease. In other words, the estimate for x_d, $\hat{x}_d$, is governed by

$$\dot{\hat{x}}_d = -\gamma(x - x^*) \tag{22}$$

where the initial condition $\hat{x}_d(0)$ is the "best guess" of x_d for a given x^*. The control law Equation (9) is now modified to

$$u^2 = \begin{cases} 0, & x > \hat{x}_d \\ k(\hat{x}_d - x), & x < \hat{x}_d \end{cases} \tag{23}$$

The steady state condition is now given by

$$T^* = \frac{\beta k_s}{\alpha}(\hat{x}_d^* - x^*) + T_r \tag{24}$$

$$\bar{K}x^* = K_{sma}\, g(T^*, \varepsilon^*, \sigma^*) \tag{25}$$

where $\hat{x}_d^*$ is the steady-state value of $\hat{x}_d$. The closed loop system is shown in the block diagram form in Figure 7.

Defining the error state as before, including an extra one for $\hat{x}_d$,

$$\delta x_d = \hat{x}_d - \hat{x}_d^*$$

The closed loop system can again be written as Equations (17), with the augmented (A, B, C) as

$$X = \begin{bmatrix} \delta T \\ \delta x \\ \delta \dot{x} \\ \delta x_d \end{bmatrix}, \quad A = \begin{bmatrix} -\alpha & -\beta k_s & 0 & \beta k_s \\ 0 & 0 & 1 & 0 \\ 0 & -\frac{\bar{K}}{M} & -\frac{B}{M} & 0 \\ 0 & -\gamma & 0 & 0 \end{bmatrix}, \tag{26}$$

$$B = \begin{bmatrix} 0 \\ 0 \\ -\frac{K_{sma}}{M} \\ 0 \end{bmatrix}, \quad C = [1 \quad 0 \quad 0 \quad 0]$$

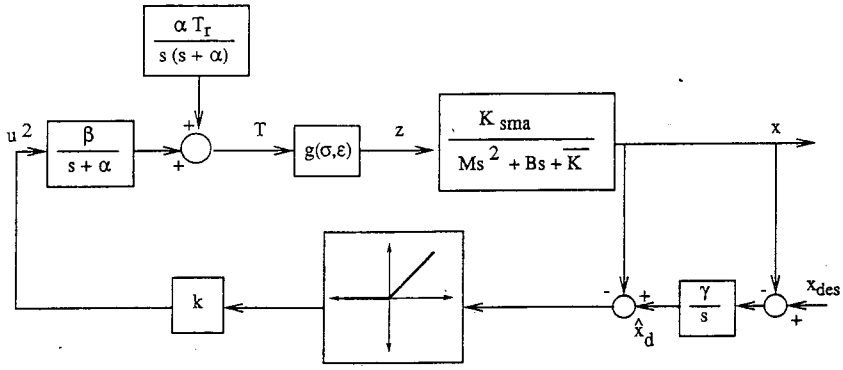

Figure 7. *Feedback block diagram of closed loop system with adaptive* x_d.

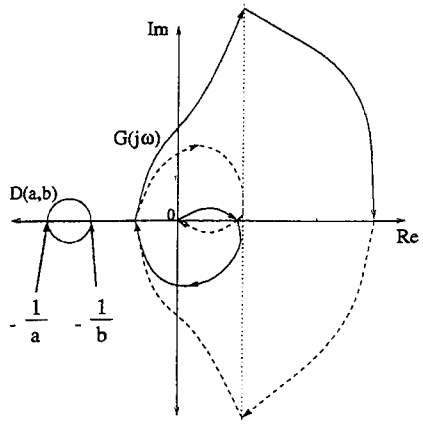

Figure 8. *Circle criterion for controller with adaptive* x_d.

The eigenvalues of A are the same as in the previous case, except that there is an additional eigenvalue at the origin. The Circle Criterion can once again be applied to check the closed loop asymptotic stability. The forward transfer function can be computed to be

$$G(s) = C(sI - A)^{-1}B$$

$$= \beta k_s K_{sma}(s+\gamma)s^{-1}(s+\alpha)^{-1}(Ms^2 + Bs + \bar{K})^{-1} \tag{27}$$

The general shape of the Nyquist plot of $G(s)$ is as shown in Figure 8. For γ sufficiently small, the intersection of the plot with the real axis is proportional to k_s. Therefore, for k [in Equation(12)] and γ sufficiently small, the closed loop system is globally asymptotically stable.

To gain some insight on the dependence of the closed loop stability on the controller parameters, a heuristic method is to apply the Mean Value Theorem and replace $\phi(\delta T)$ by $\phi'(\eta)\delta T$ [$\phi'(\eta) = K_{sma}g'(\eta)$] for some $\eta \in [0,\delta T]$. The closed loop A matrix then becomes

$$A = \begin{bmatrix} -\alpha & -\beta k_s & 0 & \beta k_s \\ 0 & 0 & 1 & 0 \\ \dfrac{K_{sma}}{M}g'(\eta) & -\dfrac{\bar{K}}{M} & -\dfrac{B}{M} & 0 \\ 0 & -\gamma & 0 & 0 \end{bmatrix}$$

Treating $g'(\eta)$ as a constant scalar, the characteristic polynomial of A is

$$\det(\lambda I - A) = M^{-1}(M\lambda^4 + (B + \alpha M)\lambda^3$$

$$+ (\bar{K} + \alpha B)\lambda^2 + (\alpha\bar{K} + g'(\eta)\beta k_s K_{sma})\lambda$$

$$+ g'(\eta)\beta k_s K_{sma}\gamma)$$

The Routh-Hurwitz Criterion can be applied to determine the stability of this system. It follows that the system would be stable if k_s and γ are chosen sufficiently small.

Extensions

There are several possible extensions of the approach presented in this paper. It is possible to replace the gain switch in Equation (12) to, for example,

$$k_s = \begin{cases} k_1, & x < x_d \\ -k_2, & x > x_d \end{cases} \tag{28}$$

Stability is assured in both fixed x_d case and adaptive case x_d if k_2 is chosen to be sufficiently small. This modification may be advantageous to weaken the spring restoration force when $x > x_d$, which, if uncompensated, may cause large overshoot, leading to large oscillations.

It is also possible to attach an opposing SMA wire to cause a push/pull type of action. If the feedback gain k is chosen to be the same for both wires, k_s can be considered as a constant irrespective of the sign of $(x - x_d)$. The stability analysis presented before also remains valid.

EXPERIMENTAL RESULTS

The controllers developed in the previous sections have been implemented on the one-link flexible beam tested. The SMA wire was connected between the hub end and the free end of the flexible beam. The strain gages on the beam were used to measure the strain.

Some experimental results were obtained using the three different controllers described in the previous sections. The desired beam strain was chosen to be 50 μstrain. Figure 9 shows the strain response for the first controller Equation (9) with $k = 30$. For each x_d, the closed loop system would reach a steady state. The corresponding x^* is recorded. This allows a monotonic map from x_d to x^* to be constructed. This map is

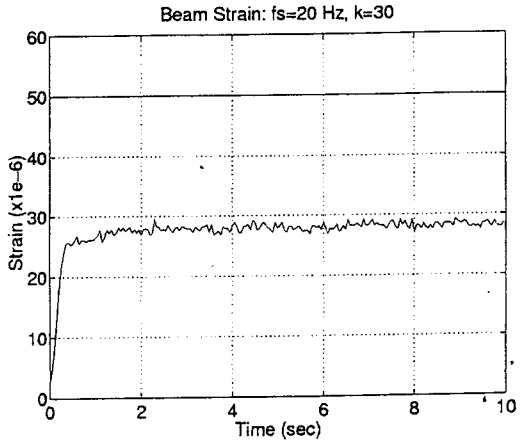

Figure 9. *Strain response: controller of Equation (9) with* k = 30.

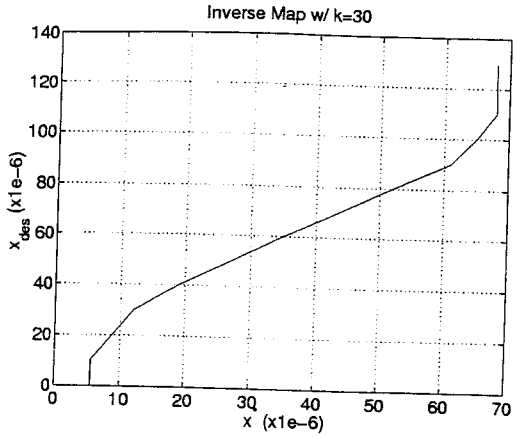

Figure 10. *Inverse mapping with* k = 30.

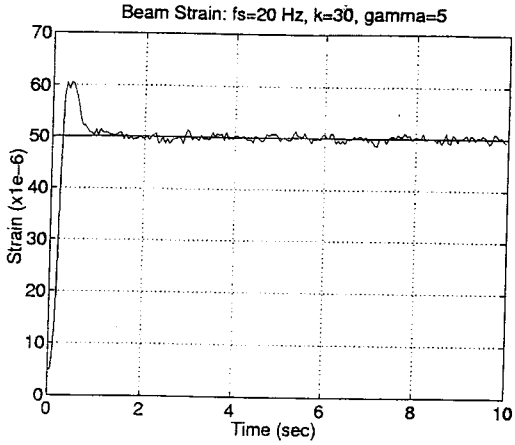

Figure 13. *Strain response: adaptive controller* (k = 30, γ = 5).

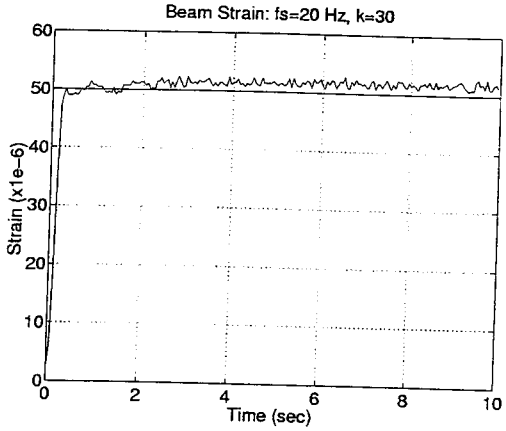

Figure 11. *Strain response: controller with mapping* (k = 30).

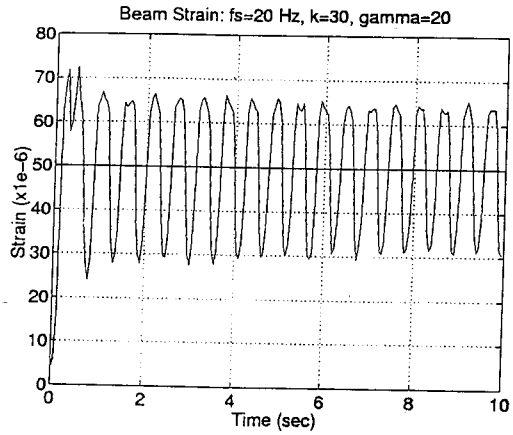

Figure 14. *Strain response: adaptive controller* (k = 30, γ = 20).

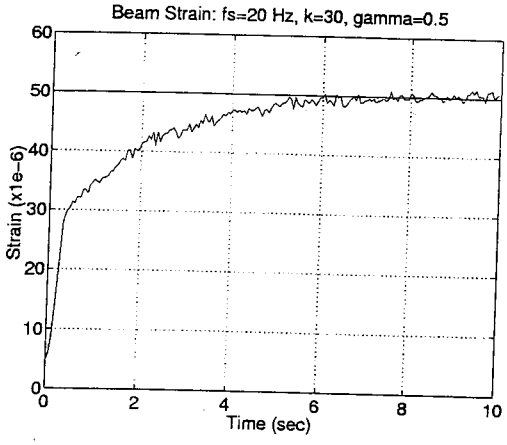

Figure 12. *Strain response: adaptive controller* (k = 30, γ = 0.5).

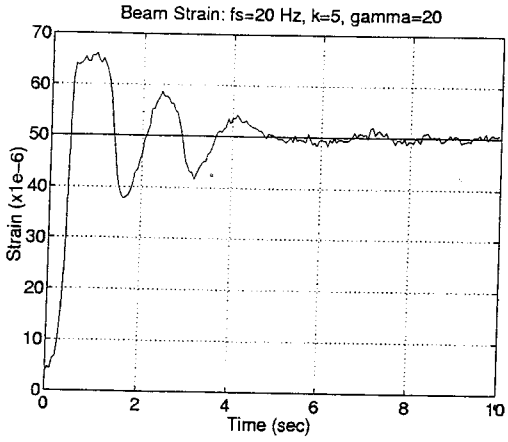

Figure 15. *Strain response: adaptive controller* (k = 5, γ = 20).

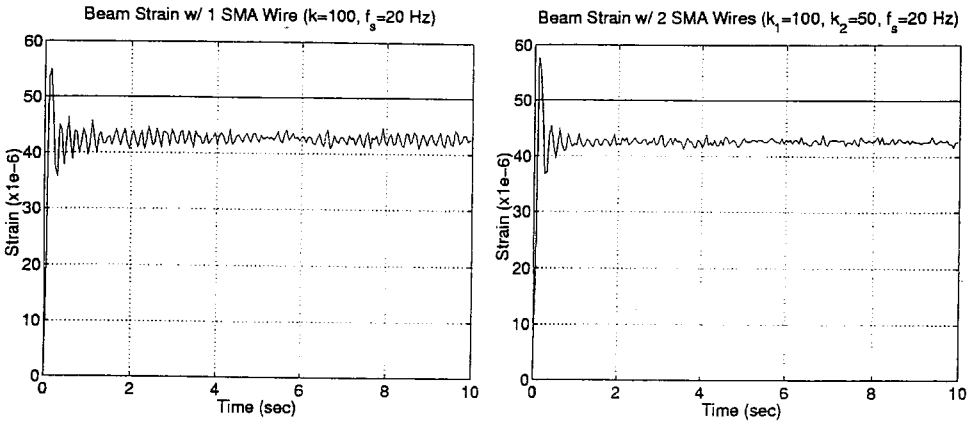

Figure 16. *Strain response: 1-wire vs. 2-wires.*

numerically inverted (see Figure 10) and used in the controller Equation (9). The experimental result shown in Figure 11 is indeed asymptotically stable as predicted. The remaining steady-state error is due to error in the inverse map.

To avoid the explicit construction of the inverse map, we apply the adaptive controller as in Equations (22) and (23). The feedback gain k remains fixed at 30. Figure 12 shows the strain response for the adaptive controller with $\gamma = 0.5$ which almost completely removes the steady-state error (as compared to the fixed x_d case). Increasing γ to 5 decreases the rise time as shown in Figure 13 (but now produces an overshoot). The steady-state error remains almost zero. Increasing the adaptive gain still further to $\gamma = 20$ causes a limit cycle type of behavior in the closed loop system (Figure 14). Using the same γ value but decreasing k to 5 (Figure 15), once again stabilizes the system. This confirms our analysis that the product of k and γ needs to be chosen sufficiently small.

Finally, an opposing SMA wire was attached to the experimental testbed to examine push/pull type of action. The feedback gains were chosen to be $k_1 = 100$ and $k_2 = 50$, where k of Equation (12) is k_1 for the first SMA wire and k_2 for the second SMA. Two different feedback gains have been used since the two SMA wires are mounted slightly differently, affecting their respective effectiveness. The experiment was run first for the fixed x_d case. When compared to the experimental result using only one SMA under the same conditions, the magnitude of the oscillations was slightly reduced (see Figure 16). Applying the adaptive case of the controller with $\gamma = 10$ produced a very small steady-state error (Figure 17). As shown in Figure 18, even further reduced oscillations can be obtained by increasing the sampling frequency.

Overall, the experimental results show excellent qualitative agreement with the theoretical analysis. The controller that uses fixed x_d produces a good result, but the mapping from x^* and x_d must be obtained for each different value of k. The adaptive controller that estimates x_d can be tuned (adjusting both k and γ) to produce good results. If the gains are chosen too high, instability may result. Preliminary experimental results look promising for using opposing SMA wires

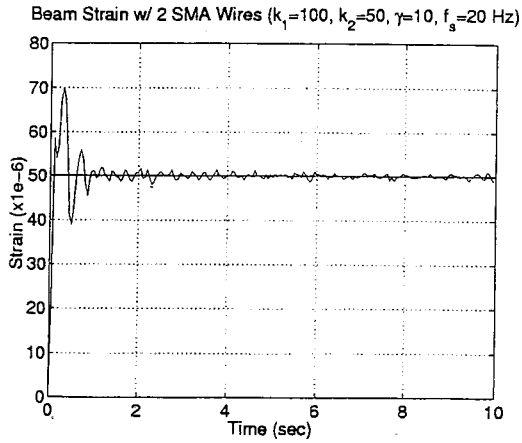

Figure 17. *Strain response: push/pull using adaptive controller.*

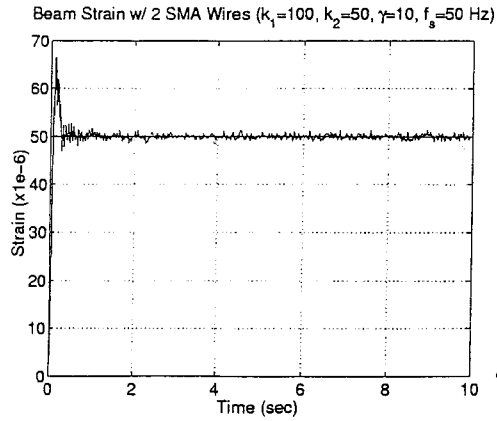

Figure 18. *Strain response: effect of sampling.*

as the results show improvement over using only a single SMA actuator.

CONCLUSIONS

SMA is an important material for smart structures because of its light weight and ability to produce relatively large force and displacement. This paper addresses the closed loop feedback control for SMA without the explicit identification of the hysteretic SMA behavior. We use a thermodynamic constitutive model of SMA combined with a single mode model of the flexible beam to qualitatively analyze the closed loop stability of the system. In our past work, we applied a nonlinear proportional feedback to the SMA system and found that for sufficiently small gain the closed loop system is stable but can have significant steady-state error. In this paper, we modify the controller to include a mapping that compensates for the steady-state error and show that the closed loop system is globally asymptotically stable. However, the required mapping must be calculated or identified for each different controller gain. This requirement is removed by further modifying our controller to include an adaptive update for the steady-state value of the displacement output. The closed loop system is again shown to be globally asymptotically stable provided that the gains are chosen sufficiently small. Experiments in our laboratory confirm the qualitative analysis for each of the controllers. Though the analysis in this paper is based on set point control, the set point can be made time varying for trajectory tracking. We have experimentally shown that the closed loop bandwidth is approximately 1–2 Hz.

ACKNOWLEDGEMENT

The authors acknowledge the financial support of the Army Research Office, grant DAALO3-92-G-012. The first author acknowledges the financial support of the National Science Foundation for her Graduate Research Fellowship.

REFERENCES

Baz, A., Imam, K., and McCoy, J. (1990). Active vibration control of flexible beams using shape memory actuators. *Journal of Sound and Vibration*, 140(3):437–456.

Dickinson, C. (1997). *Feedback Compensation of Shape Memory Alloy Hysteresis.* Doctoral thesis, Rensselaer Polytechnic Institute, Troy, NY.

Dickinson, C. A., Hughes, D. C., and Wen, J. T. (1996). Hysteresis in shape memory alloy actuators: the control issues. In *Proceedings of the 1996 Mathematics and Control in Smart Structures Conference,* pages 494–506, San Diego, CA.

Grant, D. and Hayward, V. (1997). Controller for a high strain shape memory alloy actuator: Quenching of limit cycles. In *Robotics and Automation Conference,* pages 254–259.

Hughes, D. and Wen, J. (1995). Preisach modeling of piezoceramic and shape memory alloy hysteresis. In *Proc. IEEE Conference on Control Applications,* pages 1086–1091, Albany, New York.

Ikegami, R., Wilson, D. G., Anderson, J. R., and Julien, G. J. (1990). Active vibration control using nitinol and piezoelectric ceramics. *J. of Intell. Mater. Syst. and Struct.*, 1:189–205.

Madill, D. R. and Wang, D. (1994). The modelling and L_2-stability of a shape memory alloy position control system. In *Robotics and Automation Conference,* pages 293–299.

Shu, S. G., Lagoudas, D. C., Hughes, D., and Wen, J. T. (1997). Modeling of a flexible beam actuated by shape memory alloy wires. *Smart Mater. Struct.*, 6:265–277.

Vidyasagar, M. (1993). *Nonlinear Systems Analysis.* Prentice Hall, New Jersey, 2nd edition.